Proceedings of 2023 IEEE
International Conference on Mechatronics and Automation
August 6 - 9, Harbin, Heilongjiang, China

Study on Control Strategy of the Vascular Interventional Surgical Robot Based on LADRC

Wenqiang Zhang[1], Jian Guo[1,2*]

[1] Tianjin Key Laboratory for Control Theory & Applications In Complicated Systems and Intelligent Robot Laboratory

*Tianjin University of Technology Binshui Xidao Extension 391, Tianjin, 300384,China 1071791881@qq.com; *Corresponding author: jianguo@tjut.edu.cn;*

Shuxiang Guo[1,2,3*]

[2]Shenzhen Institute of Advanced Biomedical Robot Co., Ltd.

*No.12, Ganli Sixth Road, Jihua Street, Longgang District, Shenzhen,518100, China *Corresponding author: guoshuxiang@hotmail.com;*

and Qiang Fu[1]

[3] Key Laboratory of Convergence Medical Engineering System and Healthcare Technology, The Ministry of Industry and Information Technology, School of Life Science

Beijing Institute of Technology No.5,Zhongguancun South Street,Beijing,100081,China fuqiang6369@hotmail.com

***Abstract* - As a medical device used in surgery, the vascular interventional surgical robot itself needs to have good control accuracy to ensure the safety of the surgery process. Given this security problem, this paper selects the Line Active Disturbance Rejection Control (LADRC) as the control strategy of the vascular interventional robot, aiming at improving the master-slave tracking accuracy of the vascular interventional robot. This article compares the LADRC and PID(Proportional-Integral-Derivative) control strategies through simulation and experiments. The experimental results show that LADRC has good control performance for master-slave tracking and can be applied to the vascular interventional surgical robots.**

***Index Terms* - medical device, vascular interventional surgical robot, control accuracy, Line Active Disturbance Rejection Control(LADRC), control strategy**

I. INTRODUCTION

In recent years, people's daily routines have become more chaotic compared to the last century. Due to the continuous changes in people's living environment and the increasing pace of life, the physical mechanisms of most citizens have been in an overloaded state. Many chronic diseases have gradually become the mainstream diseases endangering the physical health of our citizens, and even gradually tend to be younger. Cardiovascular diseases are a perennial threat to the physical health of modern humans, and the number of deaths caused by cardiovascular diseases in China is still increasing yearly.

Professor Huo Yong of Peking University First Hospital recently released the treatment data of Percutaneous Coronary Intervention (PCI) in the Chinese Mainland at the 25th China Cardiovascular Intervention Forum[1]. Due to the impact of the novel coronavirus in 2020, the overall situation of interventional surgery in the Chinese Mainland has fluctuated slightly. In addition, the number of PCI surgeries has been increasing yearly. Robot technology is widely used in various industries and fields in the 21st century. The full integration of robot technology and the medical field has greatly promoted the intelligent research and development of medical devices. Interventional surgery robots have broken traditional interventional surgery operation conventions, and doctors and interventional surgery robots can cooperate remotely to complete interventional surgery operations.

Many domestic researchers have adopted different research methods to study the accuracy of interventional surgery robots. In 2017, researchers from the Intelligent Robotics Laboratory of Tianjin University of Technology researched master-slave tracking using the fuzzy PID control strategy[2]. In 2019, Professor Guo from the Beijing University of Technology proposed a PID fuzzy logic controller for master-slave tracking[3]. In 2021, Professor Guo Jian's team from Tianjin University of Technology proposed using the self-coupling PID control method for master-slave tracking[4]. In the same year, the research team again proposed an algorithm combining fuzzy PID and improved Smith estimation compensation to conduct in-depth research on master-slave tracking[5]. Li Yifa of the Beijing University of Posts and Telecommunications proposed using PID fuzzy controllers for master-slave tracking control[6].

In interventional surgery, the accuracy of master-slave tracking is very important. The innovation of this article is to use LADRC method and improve the master-slave tracking accuracy of the interventional robot to ensure safe operation. This article is divided into five parts. The first part introduces the background and significance of interventional surgery and the research status of interventional surgery robots; The second part introduces the interventional surgery robot platform; The third part builds the simulation environment through Simulink in MATLAB (2022b); The fourth part will conduct experiments and analysis on position tracking between the master and slave operators; The fifth part will summarize this article.

II. OVERVIEW OF SYSTEM PLATFORM

This article's vascular interventional surgery robot adopts a master-slave control mode. The interventional surgery robot system is divided into the master operator and the slave operator. Considering the habit of surgeons operating guide

979-8-3503-2084-8/23/$31.00 ©2023 IEEE

wires and catheters during daily interventional surgery and meeting the need for doctors to maintain a sense of touch when operating interventional surgery robots, the main end operator adopts two magnetic rods for coaxial delivery and rotation of the guide wires and catheters and utilizes the principle of electromagnetic induction to achieve the force feedback function of the master and slave ends. The slave operator uses a linear displacement unit with multiple grippers to replace the human hand in the axial and radial motion of the wire guide, achieving delivery and rotational motion of the wire guide. When the surgeon operates the master operator, the linear displacement sensor and rotary encoder in the master operator transmit the collected signal to the microcontroller. After receiving the signal transmitted by the microcontroller, the slave operator drives a stepper motor to push or rotate the guide wire and catheter, replicating a series of operations of the master operator on the guide wire and catheter[7].

The overall conceptual diagram of an interventional surgery robot is shown in Fig.1. The physical drawing of the main operator is shown in Fig.2, and the physical drawing of the slave operator is shown in Fig.3.

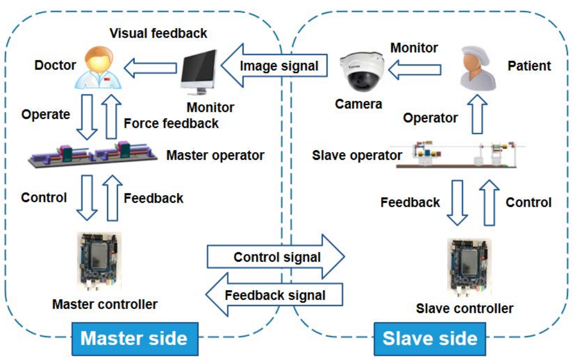

Fig. 1 Concept diagram of vascular interventional surgery robot

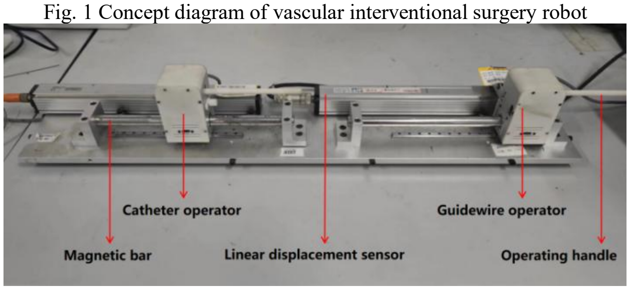

Fig. 2 The master manipulator

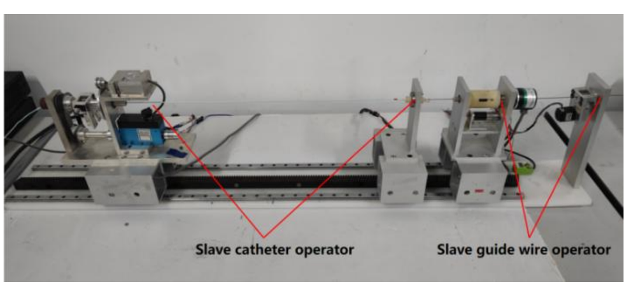

Fig. 3 The slave manipulator

III. Comparison of Controling Strategies

A. Traditional PID control strategy

As one of the oldest and most widely used control methods in the development of industrial production, classical PID control is still enduring until various control strategies emerge endlessly today. Classical PID control has significant advantages such as simple control principles. The structure diagram of classical PID control is shown in Fig.4.

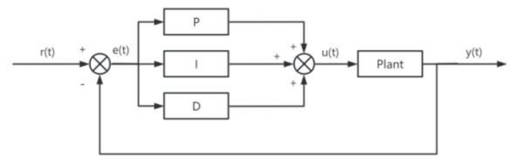

Fig. 4 Structure diagram of classical PID control

The general rule of classical PID control is:

$$\mathrm{u}(t) = k_P\left[error(t) + \frac{1}{T_I}\int_0^t error(t)dt + \frac{T_D derror(t)}{dt}\right] \quad (1)$$

Where k_P is the proportional coefficient, T_I is the integral time constant, and T_D is the differential time constant[8].

Although classical PID control has significant effects, there are still many disadvantages:

Tracking a given variable that may experience mutations is unreasonable using continuously changing output variables. It is difficult to find a suitable Differentiator to extract differential signals; The PID controller is a linear combination of proportional, integral, and differential effects. This linear combination method may not be the most suitable; When there is no disturbance in the system, the integration link will affect the system's dynamic characteristics, such as slowing the response of the closed-loop system.

B. LADRC control strategy

Automatic disturbance rejection control technology inherits the essence of PID control. Han Jing Puritan officially proposed this technology in the 1990s and is commonly called non-linear ADRC technology.

Professor Han attributes the core part of the control problem to a disturbance rejection problem. He proposed four improvements: using an extended state observer to estimate the total disturbance of the system; Arranging transition processes to reduce overshoot of the system; Using tracking differentiators to achieve reliable acquisition and smooth output of differential signals; A nonlinear state error feedback strategy is used to improve the efficiency of feedback control. The central idea of nonlinear ADRC is to take the simple integral series type as the standard type, treat the parts of the system dynamics that are different from this standard type (including system uncertainties and disturbances) as total disturbances (including internal and external disturbances), and use the extended state observer as a means to estimate and eliminate the total disturbances in real-time[9]. Its basic control structure diagram is shown in Fig.5.

As can be seen from the above figure, the active disturbance rejection controller is specifically divided into the following three parts: an extended state observer (ESO), a Tracking differentiator (TD), and Nonlinear State Error Feedback (NLSEF)[10].

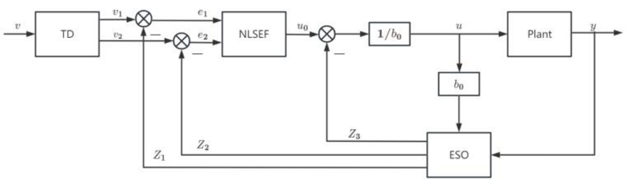

Fig. 5 Structure diagram of the nonlinear ADRC

The nonlinear ADRC requires too many parameters to be adjusted, and the control is relatively complex in practical application environments. Professor Gao Zhiqiang from Cleveland State University, proposed the concept of frequency scale and found that using linear functions can still obtain controllers with good control effects. Therefore, a control theory of linear active disturbance rejection (LADRC) technology emerged when required. The LADRC can greatly reduce the complexity of parameter tuning and meet engineering needs. He proposed simplifying the extended state observer in ADRC to a linear extended state observer, and taking the bandwidth of the linear extended state observer as its only adjustable parameter, making the design of ESO easier. In addition, in terms of controllers, Professor Gao adopts a combined form of PD control, associating the proportional and differential coefficients with the controller's bandwidth and making the controller's bandwidth the only adjustable parameter[11].

Taking a second-order system as an example, the basic structure of a linear active disturbance rejection controller mainly includes two parts: a linear extended state observer (LADRC) and a PD controller. The specific structure is shown in Fig.6[12].

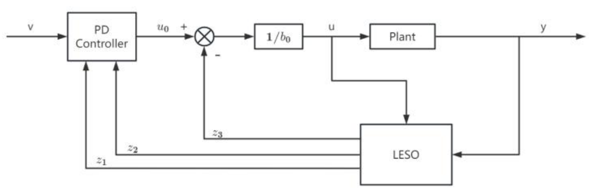

Fig. 6 Structure diagram of the LADRC

Because ADRC is almost completely independent of the precise model of the controlled object, the linear extended state observer estimates the expanded system state through the input and output signals of the system.

Assume that the second-order controlled object:

$$\ddot{y} = f(y, \dot{y}, w, t) + bu = -a_1\dot{y} - a_0 y + w + bu \quad (2)$$

Where, y and u represent the output and input signals of the system, a_0 and a_1 represent unknown coefficients, w represents the external disturbance of the system, b is partially known (where the known part is recorded as b_0),

Therefore, the above formula can be changed to:

$$\ddot{y} = -a_1\dot{y} - a_0 y + w + (b - b_0)u + b_0 u = f + b_0 u \quad (3)$$

Where f represents the total disturbance of the system, including internal disturbances and external disturbances, including the system.

Selecting the state variable: $x_1 = y$, $x_2 = \dot{x}_1 = \dot{y}$, $x_3 = f$, $\dot{x}_3 = \dot{f} = h$.

Therefore, the continuous state space of the system is described as:

$$\begin{cases} \dot{x} = Ax + Bu + Eh \\ y = Cx \end{cases} \quad (4)$$

The continuous linear extended state observer (LESO) of the system is established in the following form:

$$\begin{cases} \dot{z} = Az + Bu + L(y - \hat{y}) = Az + Bu + L(y - Cz) \\ \hat{y} = Cz \end{cases} \quad (5)$$

Because h is unknown and can be estimated through correction terms, the above equation is ignored, and a new observer equation is obtained:

$$\begin{cases} \dot{z} = (A - LC)z + \begin{bmatrix} B & L \end{bmatrix} \begin{bmatrix} u \\ y \end{bmatrix} \\ \hat{y} = Cz \end{cases} \quad (6)$$

The gain matrix form of the linear extended state observer in the above equation is defined as follows:

$$L = [L_1 \ L_2 \ L_3]^T \quad (7)$$

To ensure the stability of the observer, the characteristic roots in the characteristic equation are placed at the same location at $-\omega_o$ through pole placement, ω_o ($\omega_o > 0$) is the bandwidth of the linearly expanded state observer.

Therefore[13]:

$$L = \left[3\omega_o, 3\omega_o^2, \omega_o^3\right]^T \quad (8)$$

Therefore, as long as the appropriate bandwidth of the linear extended state observer is selected, the linear extended state observer can be obtained through a unique correspondence with the observer gain matrix. The structure of the extended state observer for the second-order system LADRC is shown in Fig.7[14-15].

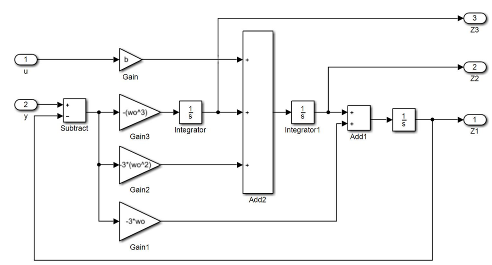

Fig. 7 Structure diagram of the extended state observer

Professor Gao's team used a linear combination of traditional PID controllers to design the controller; the linear state error feedback control law is simplified to a PD combination.

For the following second-order controlled objects:

$$\ddot{y} = f(y, \dot{y}, w(t), t) + bu \quad (9)$$

Which u represents the input signal of the system, $w(t)$ represents the external disturbance of the system, and $f(y, \dot{y}, w(t), t)$ represents the total disturbance of the system.

The control amount of a linear auto disturbance rejection controller is defined as:

$$u = \frac{u_0 - z_3}{b_0} \quad (10)$$

Where z_3 is the estimate of the total disturbance of the system by a linear extended state observer.

At this point, the system becomes a dual integrator series type:

$$y'' \approx u_0 \tag{11}$$

Therefore, the PD controller used for linear ADRC is in the following form:

$$u_0 = k_p(r - z_1) + k_d(\dot{r} - z_2) + \ddot{r} \tag{12}$$

In the formula, r represents the given value of the system, k_d is the amplification coefficient of the differential action (D), and k_p is the amplification coefficient of the proportional action (P).To avoid the adverse effects of rapid changes in a given value on system oscillations, the expression $k_d(\dot{r} - z_2)$ is replaced by $-k_d z_2$ and ignored $\ddot{r}$.

Therefore:

$$y'' = k_p(r - z_1) - k_d z_2 \tag{13}$$

So the poles of the closed-loop characteristic root are placed at the same position $-\omega_c$ (ω_c is the bandwidth of the PD controller， $\omega_c > 0$) through pole placement.

The solution is： $k_d = 2\omega_c$, $k_p = \omega_c^2$.

The PD controller for the LADRC of a second-order system is shown in Fig.8.

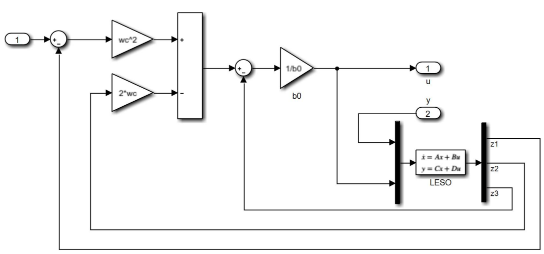

Fig. 8 Structure diagram of the PD controller

In this way, the linear simplified ADRC by Professor Gao's team only needs to set three parameters (b_0 , ω_o , ω_c), which greatly reduces the difficulty of parameter adjustment for nonlinear auto interference rejection technology.

C. Simulation under MATLAB environment

In this section, the simulation diagrams of the interventional surgery under the control strategies of PID and LADRC are built using the MATLAB(2022b).

For the previous work of our laboratory team, we can simplify the interventional surgery robot into the following second-order system.

$$G(s) = \frac{1}{1.2s^2 + 8s + 1} \tag{14}$$

With the help of Simulink simulation tools, two control strategies, PID and LADRC, were used to build simulation model diagrams. Considering the existence of external disturbances, the input signal was a step signal. To verify the anti-disturbance performance, a step signal with an amplitude of 1 was added to the control system as a disturbance, with a disturbance start time of 5 seconds, and acquisition noise with a noise power of 10^{-14} was added to the data acquisition port, as shown in Fig.9.The simulation model of the system under two control strategies are shown in Fig.10 and in Fig.11.

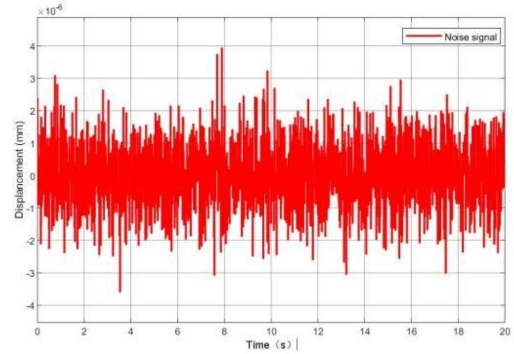

Fig. 9 Diagram of the acquisition noise signal

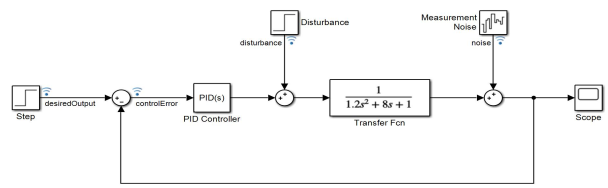

Fig. 10 Structure diagram of the PID

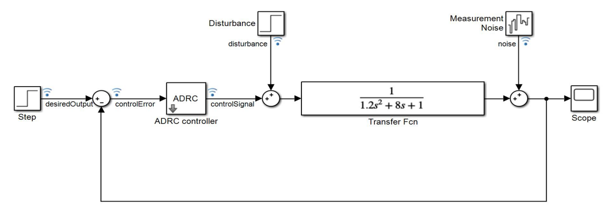

Fig. 11 Structure diagram of the LADRC

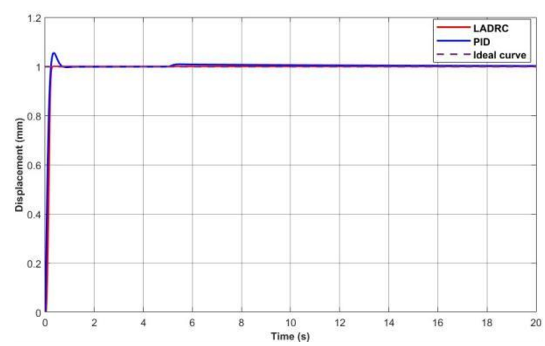

Fig. 12 Comparison diagram of LADRC and PID control

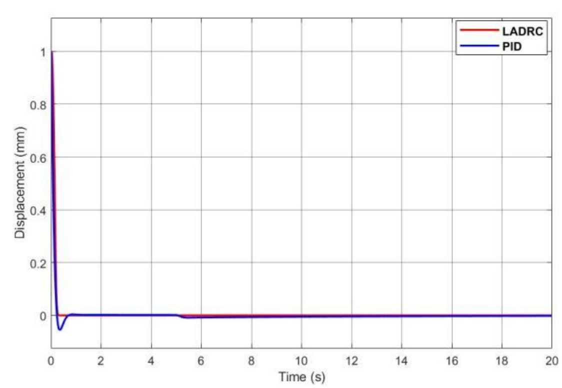

Fig. 13 Comparison diagram of LADRC and PID control error

The input amplitude of the step signal is set to 1 rad/s. The operating time is set to 20 seconds, setting the PID parameter Kp to 100, setting Ki to 10, setting Kd to 8. Setting the LADRC parameter b_0 to 0.3, setting ω_c to 50, setting ω_o to 500. The control effects of PID and LADRC on the system in the presence of disturbances are shown in Fig.12.The control error comparison diagram is shown in Fig.13.

According to the above simulation results of the two control strategies, the control performance indicators can be obtained, as shown in Table I.

TABLE I
LADRC AND PID PERFORMANCE INDEX

Control strategy	Peak time	Overshoot	Regulating time	Disturbance response
PID	0.35s	5.575%	0.54s	0.8%
LADRC	0.31s	0.0%	0.245s	0.1%

From the comparison of the above data, it can be seen that the LADRC control method has a faster corresponding speed. Moreover, for the same disturbance, the LADRC control can improve the system's anti-interference performance, and the recovery performance for system interference is stronger than the PID control strategy.

IV. EXPERIMENTS AND RESULTS

The experimental platform built for this experiment is shown in Fig.14.

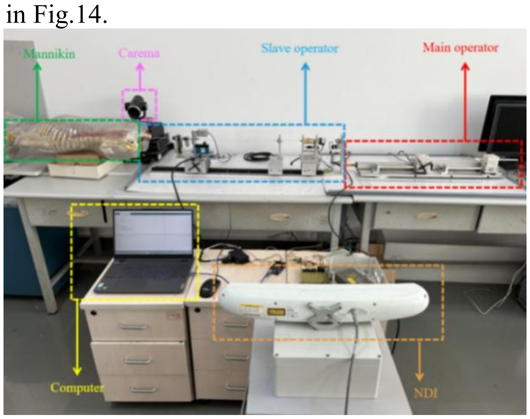

Fig. 14 The experiment of master-slave displacement

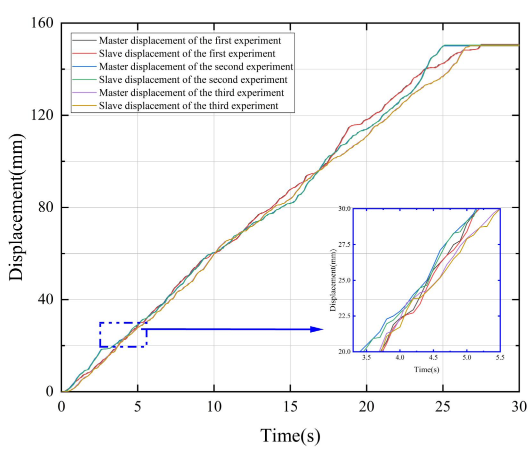

Fig. 15 The master and slave displacement experiment of LADRC

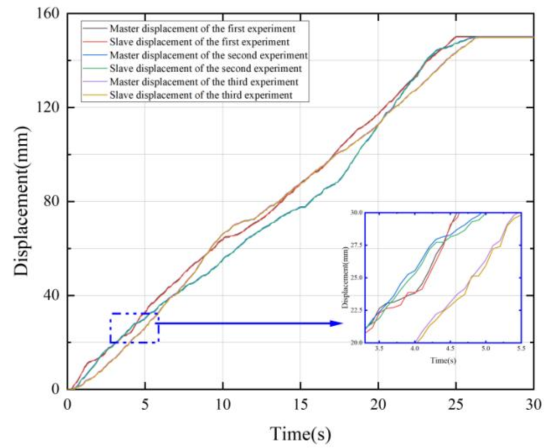

Fig. 16 The master and slave displacement experiment of PID

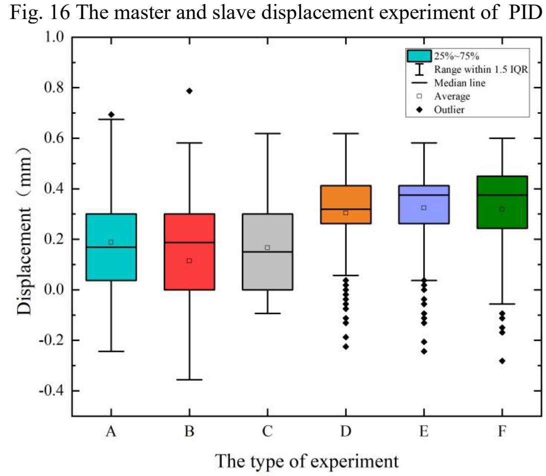

Fig. 17 The displacement error comparison between LADRC and PID

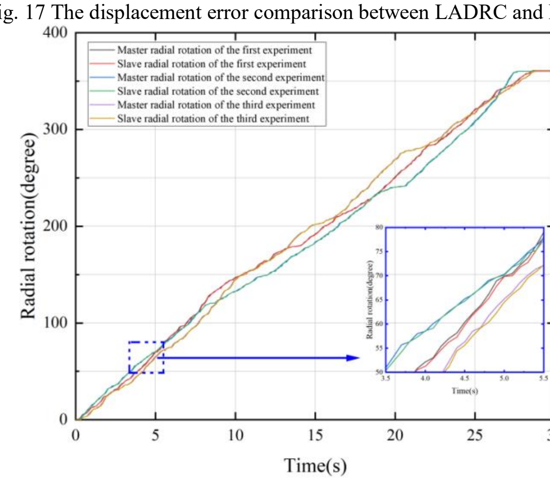

Fig. 18 The radial rotation experiment of LADRC

The catheter used in the experiment is Torcon NB produced by Cook Company in the United States ® Advantage Catheter, conduit model 5F, inner diameter 1.2mm, outer diameter 1.67mm. Using the NDI optical positioning and tracking system as a collection device for displacement information, the NDI optical tracking camera captures the motion coordinate changes of two inductive rigid bodies to reflect the position-tracking situation of the master and slave operators.

Setting the PID controller parameter Kp to 50, setting Ki to 3, setting Kd to 6. Setting the LADRC controller parameter

b_0 to 1, setting ω_c is set to 8, setting ω_o to 30. To verify the accuracy of master-slave tracking, repeat each of the following experiments three times.The master operator was used to approximately uniformly push the catheter forward by 150mm within 30 seconds. The experimental results of the two control strategies are shown in Fig.15 and Fig.16. The error comparison chart is shown in Fig.17. Experiments A, B, and C use the LADRC strategy, while experiments D, E, and F use the PID control strategy. Similarly, within 30 seconds, the catheter was approximately uniformly rotated 360 degrees. The experimental results of the two control strategies are shown in Fig.18 and Fig.19, and the radial rotation error is shown in Fig.20.

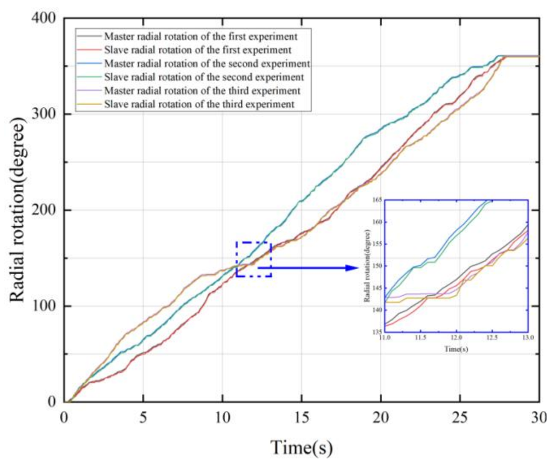

Fig. 19 The radial rotation experiment of PID

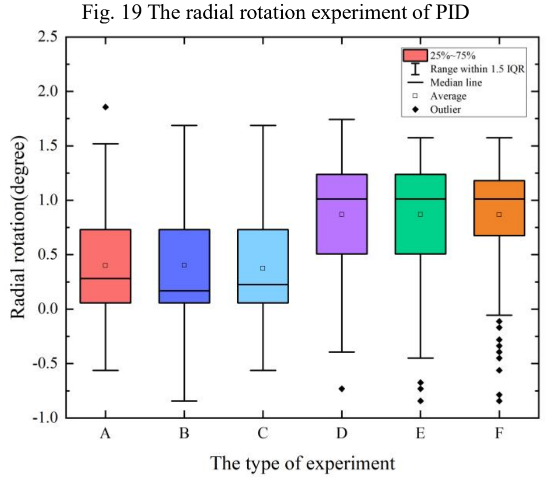

Fig. 20 The radial rotation error comparison between LADRC and PID

The above experimental data shows that the total average tracking error of the catheter using LADRC and PID control strategies are 0.16 mm and 0.315532 mm, respectively, and the total average radial rotation error is 0.39 degrees and 0.87 degrees.

V. CONCLUSIONS

This article selects Linear Active Disturbance Rejection Control (LADRC) as the control strategy for the interventional surgery robot. The simulation and experimental results show that the LADRC strategy has a significant improvement effect compared with the traditional PID control strategy in improving the control accuracy of the interventional surgery robot. In the future, we will adopt the LADRC control strategy for animal experiments with interventional surgical robots, and further apply it in practical surgeries.

ACKNOWLEDGMENT

This research is supported by the National Natural Science Foundation of China (61703305), the Key Research Program of the Natural Science Foundation of Tianjin (18JCZDJC38500), and the Innovative Cooperation Project of Tianjin Scientific and Technological (18PTZWHZ00090).

REFERENCES

[1] F. Pan, “Interventional treatment of cardiovascular diseases in China shows a good development trend”, China Modern Medicine, vol. 29, no. 21, pp. 1-4, 2022.

[2] Jian G , Jin X , Guo S , et al, “Study on the tracking performance of the vascular interventional surgical robotic system based on the fuzzy-PID controller”, 2017 IEEE International Conference on Mechatronics and Automation, 2017.

[3] S. Guo, Y. Guo, X. Bao and C. Yang, “A PID-type Fuzzy Logic Controller for an Interventional Surgical Robot”, 2019 IEEE International Conference on Mechatronics and Automation, Tianjin, China, pp. 2529-2533, 2019.

[4] Guo S, Sun Z, Guo J, “Study on Tracking Control of Vascular Interventional Surgical Robot based on Autocoupling PID”, 2021 IEEE International Conference on Mechatronics and Automation, pp. 903-908,2021.

[5] Guo J, Zhuang Z, Guo S, “Study on Delay and Accuracy of Control System for the Vascular Interventional Surgical Robot based on Fuzzy PID and Improved Smith Algorithms”, 2020 IEEE International Conference on Mechatronics and Automation, pp. 1716-1721, 2020.

[6] Y. Li, “Research on master-slave synchronous control of vascular intervention surgery robot”, Beijing University of Posts and Telecommunications, 2021.

[7] W. Zhang, J. Guo, S. Guo and Q. Fu, “Catheter Modeling And Tip Force Analysis Based On Mass Spring Model,” 2022 IEEE International Conference on Mechatronics and Automation, Guilin, Guangxi, China, pp. 774-779, 2022.

[8] Sanchis R, Peñarrocha I, “A PID tuning approach to find the optimal compromise among robustness, performance and control effort: implementation in a free software tool”, International Journal of Control, pp. 1-20, 2021.

[9] Ramírez-Neria M, Sira-Ramírez H, Garrido-Moctezuma R, et al, “Linear active disturbance rejection control of underactuated systems: The case of the Furuta pendulum”, ISA transactions, vol. 53, no. 4, pp. 920-928, 2014.

[10] Zhao Z L, Guo B Z, “On convergence of nonlinear active disturbance rejection control for SISO nonlinear systems”, Journal of Dynamical and Control Systems, vol. 22, no. 2, pp.385-412, 2016.

[11] Carreño-Zagarra J J, Guzmán J L, Moreno J C, et al, “Linear active disturbance rejection control for a raceway photobioreactor”, Control Engineering Practice, pp. 271-279, 2019.

[12] Zhang S, He L, Wang F, et al, “Generalized Predictive based Active Disturbance Rejection Control for Asymmetric Six-Phase PMSM Speed Regulation System”, 2022 IEEE 17th Conference on Industrial Electronics and Applications, pp. 446-451, 2022.

[13] Jin H, Gao Z, “On the notions of normality, locality, and operational stability in ADRC”, Control Theory and Technology, pp.1-13, 2023.

[14] Li J, Zhang L, Li S, et al, “Active Disturbance Rejection Control for Piezoelectric Smart Structures: A Review”, Machines, vol. 11, no. 2, 2023.

[15] Ran M, Li J, Xie L, “Extended state observer based reinforcement learning and disturbance rejection for uncertain nonlinear systems”, 2020 IEEE 16th International Conference on Control & Automation, pp. 1398-1403, 2020.